Available online at www.sciencedirect.com
ScienceDirect
Earth and Planetary Science Letters 256 (2007) 120–135
EPSL
www.elsevier.com/locate/epsl

Accretion of arc-oceanic lithospheric mantle in the Mediterranean: Evidence from extremely high-Mg olivines and Cr-rich spinel inclusions in lamproites

D. Prelević [a,b,*], S.F. Foley [a]

[a] Institute of Geological Sciences, University of Mainz, Becherweg 21, 55099 Mainz, Germany
[b] Department of Geochemistry, Faculty of Mining and Geology, Belgrade University, Djušina 7, 11000 Belgrade, Serbia and Montenegro

Received 2 March 2006; received in revised form 11 January 2007; accepted 16 January 2007
Available online 24 January 2007
Editor: R.W. Carlson

Abstract

Si-rich Mediterranean type lamproites (48–56 wt.% SiO_2) are olivine-phyric, mantle-derived volcanics, in which both phenocrystic and xenocrystic olivine are present. Here we demonstrate the phenocrystic origin of the most extremely NiO–MgO enriched olivine in lamproites with Mg# up to 0.95, that host Cr-rich (Cr# around 0.95) spinels. Our comprehensive study of olivine–spinel pairs from Mediterranean lamproites enables us to constrain the extent of depletion of their mantle source. Olivine–spinel pairs from primitive Mediterranean lamproites plot in the most refractory part of the olivine–spinel mantle array diagram, showing even more refractory character than mineral pairs from boninites and cratonic mantle xenoliths. This indicates involvement of an ultra-depleted mantle component which had previously lost up to 40% basaltic components. These characteristics would fit the involvement of depleted subcratonic lithospheric mantle which underwent komatiite extraction in the Archaean, but mantle of such composition and age is known neither from ultramafic xenolith suites nor in tectonically emplaced ultramafic massifs in western and central Europe. Here, we explore the possibility that the extremely depleted component of the mantle source of Mediterranean lamproites is derived from an island-arc oceanic lithosphere accreted during Alpine collisional processes. This may provide compelling evidence for recent accretion of oceanic lithospheric blocks during Mesozoic subduction–collision processes in the Mediterranean.

Keywords: ultra-depleted mantle; Spain (Vera); Italy; Balkans; postcollision; Mediterranean

1. Introduction

The Mediterranean region is a complex collage of microplates of different compositions and geological history which originated in response to late Cretaceous–Cenozoic convergence of Africa–Arabia with Eurasia when numerous continental, microcontinental and ophiolitic terranes amalgamated together. The closure of numerous pre-existing oceanic basins was facilitated by oceanic subduction, continental drift, microplate rotations and migration of subduction arcs. This complicated interaction between orogenic processes and widespread extensional tectonics gave rise

* Corresponding author. Institute of Geological Sciences, University of Mainz, Becherweg 21, 55099 Mainz, Germany. Tel.: +49 6131 39 24763; fax: +49 6131 39 23070.
E-mail address: prelevic@uni-mainz.de (D. Prelević).

0012-821X/$ - see front matter © 2007 Elsevier B.V. All rights reserved.
doi:10.1016/j.epsl.2007.01.018

to volcanism of contrasting geochemistry, which provides a potentially powerful basis for evaluating the role of different geochemical reservoirs in the geodynamic evolution of the Mediterranean.

Si-rich lamproites are one of the most distinctive mantle-derived volcanic types erupting during the Tertiary in the Mediterranean region [1]. They show some of the most extreme isotopic compositions of any mantle-derived rocks, approaching the signatures of upper crustal rocks [2,3]. Earlier workers paid particular attention to the nature and the origin of this extremely enriched mantle component. However, a strongly depleted component is indicated by very low whole-rock CaO and Al_2O_3 contents [4] as well as high-Fo olivine macrocrysts and associated Cr-rich spinel inclusions [1,5], but its origin and the geodynamic significance are not well constrained.

This paper is the first part of a comprehensive study of rocks from Mediterranean lamproitic provinces. Here, we present a study of olivine macrocrysts and spinel inclusions from Spanish, Italian, Serbian and Macedonian lamproites (Fig. 1), concentrating on the Vera lamproites, southeastern Spain. We provide evidence for a phenocrystic origin for the Mg- and Ni-rich olivines retrieved from lamproites, and argue that the composition of olivine–spinel pair is determined by the depleted component of their mantle source. We conclude that this ultra-depleted mantle component of Mediterranean lamproites may be derived from oceanic lithosphere, probably of island-arc affinity, which was accreted to the continent during Alpine collisional processes.

2. Mediterranean lamproites

Mediterranean lamproites are Si-rich lamproites, and they occur in almost all Mediterranean orogenic belts (Dinarides, Apennines, Alps, Betic Cordilleras). There is a large number of studies describing their mineralogical complexity and exceptional geochemistry ([6] and references therein). They are usually interpreted as being formed by partial melting of mixed enriched- and depleted mantle components, whereby the incompatible trace elements are dominated by the enriched end-member. Primitive members show a compositional range from 6 to 10 wt.% MgO, and from 48 to 55 wt.% SiO_2. Mediterranean lamproites, in common with the lamproites globally, show extreme enrichment in both incompatible and compatible elements as well as highly

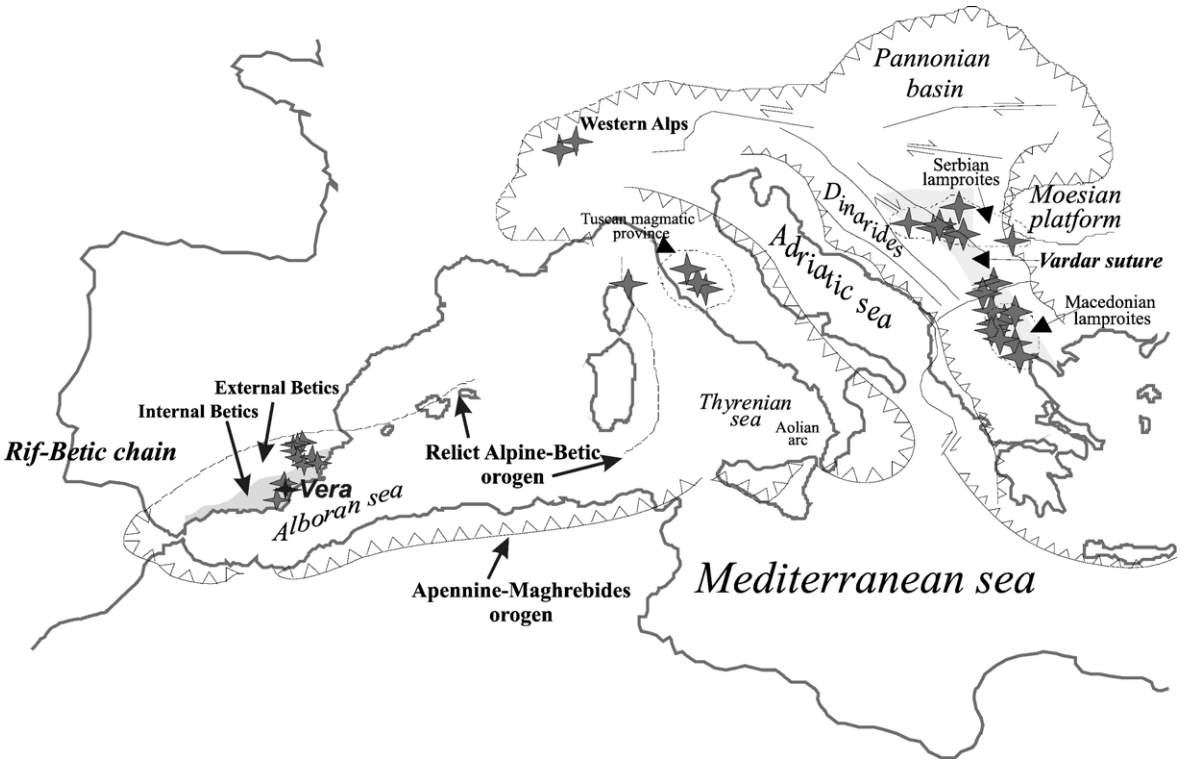

Fig. 1. Distribution of lamproites within Mediterranean (stars). Major faults are indicated by black lines. The present Apennine–Maghrebian compression front and the Alpine collision zone are also indicated.

Table 1
Representative electron microprobe analyses of phenocrystic and xenocrystic olivine together with representative analyses of Cr-spinel inclusions in both olivine populations, from the Vera (Spain) lava flow

	Sample					5-03V10		6-03V10	
	Phenocrystic olivine		Xenocrystic olivine			Cr spinel inclusions in phenocrystic olivine		Cr-spinel inclusions in xenocrystic olivine	
SiO_2	42.03	41.39	40.92	41.03	SiO_2	0.93	0.17	0.79	0.87
					TiO_2	1.06	1.17	1.15	2.05
TiO_2	0.00	0.00	0.00	0.00	Al_2O_3	3.50	3.16	6.76	7.21
Al_2O_3	0.01	0.01	0.01	0.00	FeO^T	23.33	23.52	20.55	21.34
FeO	5.46	8.31	9.66	9.47	MnO	0.24	0.28	0.30	0.24
MnO	0.04	0.13	0.17	0.12	MgO	9.04	8.47	8.13	8.54
MgO	51.69	49.72	49.64	49.25	CaO	0.02	0.06	0.25	0.16
CaO	0.09	0.11	0.05	0.06	Cr_2O_3	59.93	60.79	54.94	51.47
Cr_2O_3	0.14	0.09	0.02	0.05	NiO	0.09	0.07	0.07	0.08
NiO	0.71	0.56	0.40	0.38	ZnO	0.23	0.20	0.12	0.10
ZnO	0.00	0.08	0.01	0.00	CoO	0.05	0.04	0.04	0.06
CoO	0.04	0.05	0.02	0.02	V_2O_3	0.12	0.19	0.33	0.32
Sum	100.26	100.62	100.90	100.44	Sum	98.57	98.14	93.43	94.27
Si	1.009	1.003	0.995	0.999	Si	0.257	0.049	0.227	0.250
Ti	0.000	0.000	0.000	0.000	Ti	0.221	0.246	0.248	0.444
Al	0.000	0.000	0.000	0.000	Al	1.139	1.040	2.286	2.449
Fe	0.110	0.168	0.196	0.193	Fe^{3+}	0.756	0.854	0.132	0.271
Mn	0.001	0.003	0.003	0.003	Fe^{2+}	4.630	4.636	4.798	4.870
Mg	1.850	1.797	1.799	1.788	Mn	0.055	0.065	0.073	0.057
Ca	0.002	0.003	0.001	0.002	Mg	3.720	3.524	3.477	3.667
Cr	0.003	0.002	0.000	0.001	Ca	0.005	0.018	0.076	0.048
Ni	0.007	0.005	0.008	0.007	Cr	13.082	13.416	12.462	11.725
Zn	0.000	0.000	0.000	0.000	Ni	0.020	0.015	0.017	0.017
Co	0.000	0.000	0.000	0.000	Zn	0.047	0.040	0.025	0.020
Sum	2.983	2.989	3.002	2.994	Co	0.010	0.010	0.009	0.015
Mg#	0.944	0.914	0.902	0.903	V	0.060	0.093	0.169	0.166
					Sum	24.003	24.004	24.000	24.000

The olivine analyses are recalculated on the basis of 4 oxygen atoms per formula unit, and the Cr-spinel analyses are recalculated on the basis of 32 oxygen atoms per formula unit. Full set of microprobe analyses is given as Supplemental files 1, 2 and 3.

enriched radiogenic isotope signatures. Previous studies implied that their mantle source is distinct from the sources of the other volcanics of the area.

Two components are known to be involved in the origin of Mediterranean lamproites: (i) a crustal component, responsible for crust-like trace element patterns and radiogenic isotope systematics [7,8], and (ii) an extremely depleted mantle component characterized by very low whole-rock CaO and Al_2O_3 (much lower than in any voluminous basalts such as MORBs, tholeiites or OIBs), high-Fo olivine and Cr-rich spinel, which isotopically may resemble European SCLM [1,9]. The origin and the geodynamic significance of the depleted mantle end-member is not well constrained, probably partly because the origin of high-Mg olivine as phenocrysts has frequently been questioned [10–12].

3. Analytical methods

Major element compositions of analysed minerals and glass were determined by electron microprobe (JEOL JXA 8900RL) at the University of Mainz. Operating conditions were generally 15 kV accelerating voltage, 12 nA beam current, 1–5 μm beam diameter and 15–30 s counting time on peak. Synthetic and natural minerals were used for standardization.

Trace elements were measured using laser ablation microprobe-inductively coupled plasma-mass spectrometry (LAM-ICP-MS) at the University of Mainz using a New Wave UP-213 laser ablation system coupled to Agilent 7500ce plasma-mass spectrometer (ICPMS). The laser was operated at a repetition rate of 10 Hz and typical energies of 0.5–1 mJ per pulse, allowing data collection from individual grains in polished thick sections (100 μm) for at least 100 s. All analyses were carried out with spot diametres of 50 and 80 μm. Argon was used as the carrier gas with a flow rate of 1.2 l/min. Data collection was monitored in time-resolved format and the data were processed on-line using GLITTER software. Calibration was based on the NIST 612 trace element glass standard with reference values from [13]. Silicon was used as the internal standard for

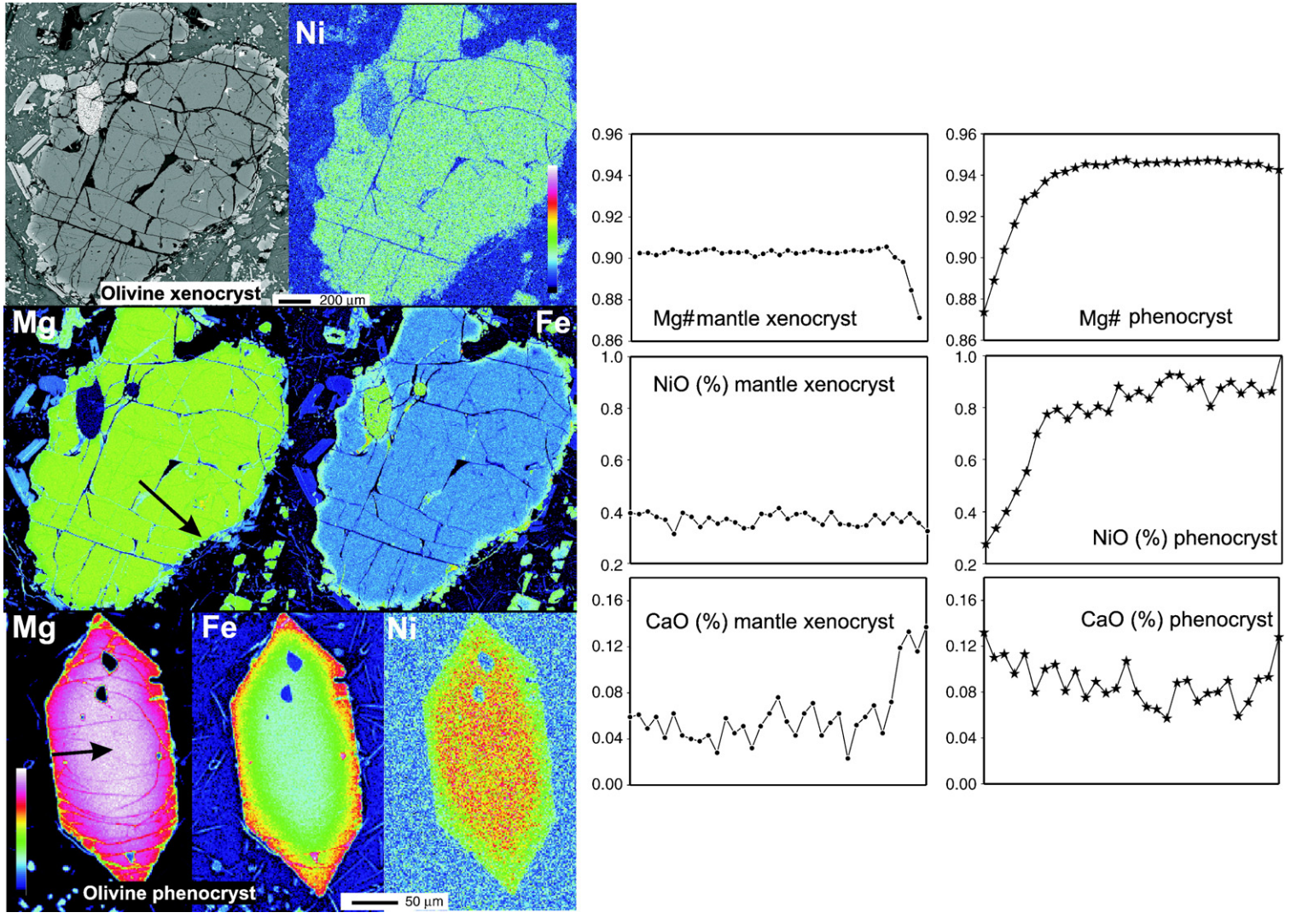

Fig. 2. Element-distribution maps and line analyses across olivine xenocryst and phenocryst from the Vera lava flow. The arrows denote analysed trends for selected grains.

Table 2
Average trace element concentrations (in ppm) for phenocrystic and xenocrystic olivine, and the glass from Vera lamproite

Element	Vera olivine phenocryst	Vera olivine xenocryst	Vera glass	Average $D^{oliv/liq}$
Li	24.64	7.91	41.03	0.600
Al	119.73	44.82	45,000	0.003
Sc	3.57	3.71	15.34	0.233
Ti	60.85	13.09	9866	0.006
V	6.90	2.48	73.45	0.094
Cr	883.36	76.53	153.57	5.752
Mn	599.79	855.53	300.03	1.999
Co	103.82	116.85	11.19	9.275
Ni	4389.26	2462.98	105.14	41.745
Cu	1.27	1.25	17.05	0.074
Zn	74.77	45.85	43.15	1.733
Ga	0.15	0.10	61.88	0.002
Sr	1.77	0.16	452.57	0.004
Y	0.14	0.03	21.91	0.007
Ce	0.16	0.08	251.96	0.001

Also, average $D^{oliv/liq}$ is given. Full set of Laser Ablation ICP-MS analyses is given as a Supplemental file 4.

quantification of olivine and glass analyses. The calibration protocol involves standardization at the beginning and end of each analytical run to correct for instrumental drift. During each run BCR2g standard glass was analysed as an unknown; accuracy and reproducibility of the analyses are given in Appendix A.

4. Sample selection and analytical strategy

We collected samples from almost all lamproitic outcrops in Spain, Italy, Serbia and Macedonia. The freshest and most primitive samples were further processed for microprobe and LAM-ICP-MS analyses. We performed more than 1000 microprobe analyses of olivine and Cr-spinel, and a number of LAM-ICP-MS analyses of olivine and glass. Attention is particularly directed to the samples from the Vera lava flow in southeast Spain (Fig. 1), because it contains one of the most compositionally extreme and complex olivine populations [14]. Here, two types of olivine macrocrysts are recognized according to textural and compositional characteristics, namely phenocrysts and mantle-derived xenocrysts. In terms of olivine population(s), the rocks from the Vera locality are more exceptional than most Mediterranean lamproites. Compositionally, however, phenocrystic olivine plots clearly on the olivine array created by other lamproitic olivines (see below).

Our analytical strategy was as follows: (1) we comprehensively analysed olivine macrocrysts and Cr-spinel inclusions from about 20 selected lamproitic samples from Spain, Italy, Serbia and Macedonia; (2) we focus our attention on the two olivine populations from the Vera lava, where we thoroughly analysed a number of grains from both populations, in order to compare their compositions; (3) we also measured partition coefficients for a number of elements between glass and olivine phenocrysts in the lamproites from Vera.

5. Results

Representative microprobe analyses of olivine and Cr-spinel from Vera lamproites, including both populations, are given in Table 1. The complete dataset that includes analysed olivine macrocrysts and Cr-spinel inclusions from the selected lamproitic samples from Spain, Italy and Macedonia is reported in Supplemental files 1, 2 and 3. All these data appear on our plots, together with data from Serbian lamproites, which are published earlier [9].

The most primitive samples of Mediterranean lamproites are ubiquitously olivine-phyric, containing millimetre-sized olivines with extremely high-Fo and Cr spinel inclusions (Mg# up to 95 and Cr# around 98; see below). Phlogopite and clinopyroxene phenocrysts are also common. Textural evidence shows that Cr-spinel and high-Mg olivine are the first minerals in the crystallization sequence, in most cases preceding phlogopite and Cpx.

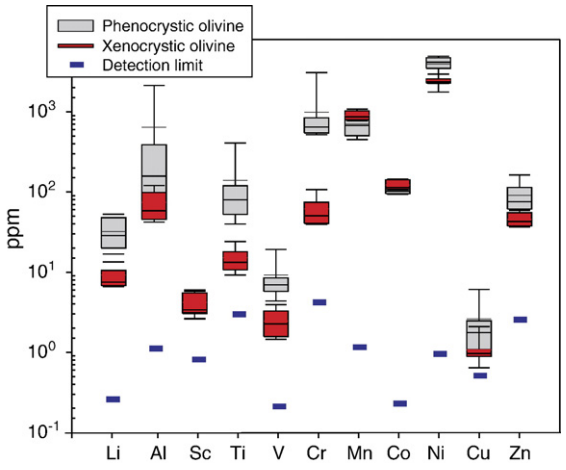

Fig. 3. Variation of trace elements in the two olivine groups identified in the Vera lava flow: phenocrystic olivine (grey; $n=11$) and xenocrystic olivine (red; $n=12$). The box depicts the central part of the sampling distribution, approximating the 25th and 75th percentile. The line across the box displays the median value. Lines extending from the box represent the range of observed values between the 10th and 90th percentile. (For interpretation of the references to colour in this figure legend, the reader is referred to the web version of this article.)

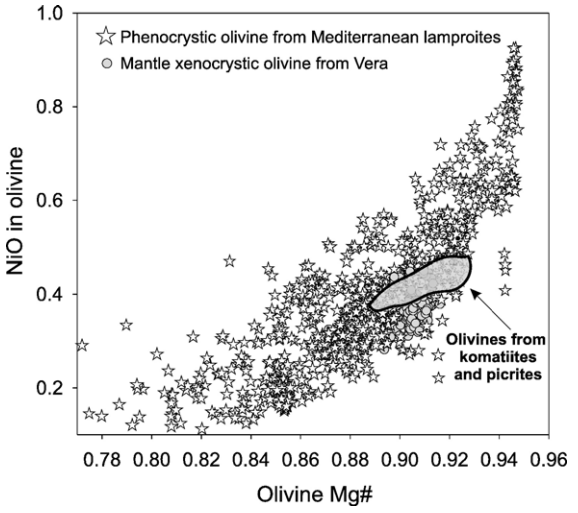

Fig. 4. Plot of olivine Mg# versus NiO for olivines from selected samples of Mediterranean lamproites. Olivines from Serbian lamproites from [9]. Data for olivine from picrites and komatiites are from the GEOROC database (HTU http://georoc.mpch-mainz.gwdg.de/georoc/UTH).

The two types of olivine macrocrysts from the Vera lava flow show considerable compositional differences (Fig. 2):

(i) Tabular idiomorphic olivine phenocrysts up to 1.0×0.3 mm have extremely high Mg# (up to 0.95) and very high NiO contents (up to 1 wt.%; Fig. 2). Cr_2O_3 (<0.18 wt.%) and CaO contents (mostly <0.20 wt.%) are low. Line analyses across selected grains show that the majority of the grains have high-Fo cores with normally zoned rims and steep compositional profiles (Fig. 2). Mg-chromite inclusions in olivine comprise tiny (<5 μm) idiomorphic crystals; they are dominated by magnesiochromites with Cr/Cr+Al reaching up to 0.98 and Fe^{2+}# 0.30–0.70 (Fe^{2+}#=Fe^{2+}/(Fe^{2+}+Fe^{3+}), with Fe^{2+} calculated from stoichiometry).

(ii) In contrast, mm-sized xenomorphic mantle olivine xenocrysts have Mg# contents not exceeding 0.92, NiO contents less than 0.4 wt.% (Fig. 2) and CaO contents not more than 0.1%. Chrome-spinel inclusions are up to 200×100 μm (Fig. 2) and have less Cr and more Al_2O_3 relative to spinel hosted by phenocrystic olivine, resulting in considerably less refractory compositions with Cr#=0.78 to 0.88.

Average trace element concentrations for phenocrystic and xenocrystic olivine, and the glass from Vera lamproite are given in Table 2. Full set of Laser Ablation ICP-MS analyses is given as a Supplemental file 4, and presented in Fig. 3. In terms of measurable trace elements, phenocrystic olivine is richer in almost all trace elements than xenocrystic olivine, including Li, Al, Cr, V, Ni, Cu and Zn. We also measured glass of the Vera lavas in order to determine trace element partitioning between olivine and melt (Table 2). Average partition

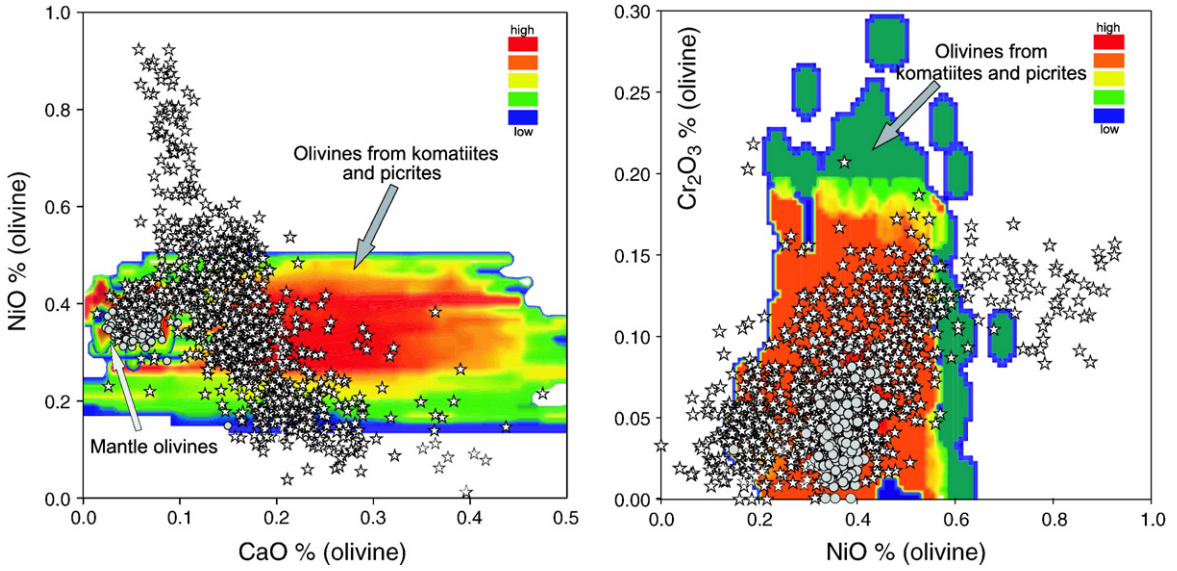

Fig. 5. Plot of CaO versus NiO and NiO versus Cr_2O_3 for olivines from selected samples of Mediterranean lamproites. Olivines from Serbian lamproites from [9]. Arrays for olivine from picrites, komatiites and peridotites are displayed as coloured density diagrams contoured from more than 1000 data points. Sources are from the GEOROC database (HTU http://georoc.mpch-mainz.gwdg.de/georoc/UTH). The symbols like in Fig. 4.

coefficients calculated from unrounded concentrations in olivine and glass are listed in Table 2.

Our whole dataset for olivine macrocrysts from Mediterranean lamproites is plotted in Figs. 4 and 5 in order to illustrate their compositional range. Olivine macrocrysts form an array distinct from komatiitic, picritic, and basaltic olivines due to systematically lower CaO and higher NiO contents. However, xenocrystic olivines from Vera clearly overlap with the compositional field of mantle olivine. Some analyses of lamproitic olivines clearly plot in the mantle olivine array characterized by the low-Ca intermediate NiO contents (Fig. 5), indicating that they probably also originated as mantle olivines, but equilibrated during reaction with the host magma. This is also clear evidence for the presence of a xenocrystic population in other localities where a clear distinction in terms of olivine morphology is lacking. The phenocrystic origin for the high-Fo high Ni olivine is, however, unambiguous.

6. Discussion

6.1. Lamproite conundrums

Numerous studies have focused on the origin of lamproites, resulting in diverse models for their origin, particularly for the silica-rich types known as leucite lamproites [15] or phlogopite lamproites [6]. There is general agreement that a normal four-phase peridotitic mantle cannot represent their source, because a K-rich hydrous mineral, in most models phlogopite, is required [16]. Moreover, experimental studies indicated that neither phlogopite–lherzolite nor phlogopite harzburgite are appropriate sources for Si-rich lamproites [16,17]. These requirements, together with the major element "depletion" and incompatible element enrichment of lamproites [18], are most easily explained by source regions composed of mixed rock types consisting partly of peridotite, which might be responsible for most of the major element composition, and partly of K-bearing ultramafic domains (veins) which contain minerals that need not be in geochemical or isotopic equilibrium with peridotite minerals [9,16]. The hydrous component in the veins is essential in order to enable melting in an otherwise refractory mantle environment. This model is in accordance with the two isotopic components recognized in the compositional spectrum of Mediterranean lamproites [1,9], whereby the enriched component has crustal-like Sr, Nd and Pb isotopes. Furthermore, the extreme enrichment in "incompatible" trace elements requires their sequestration in a number of trace phases which probably differ between localities [19].

However, much less agreement exists about the following issues:

1. The depth of partial melting to produce high-Si lamproites;
2. The origin of extremely high-Mg–NiO olivines;
3. The origin and geodynamic significance of the depleted mantle end-member.

There appears to be a close relationship between these three issues, particularly regarding the interpretation of the origin of the ultradepleted component recognized in lamproites. We concentrate on these issues in the following sections.

6.1.1. Olivine stability in the genesis of Si-rich lamproites: constraints on the depth of partial melting

There is considerable disagreement about the depth of partial melting for the Si-rich lamproites. Based on liquidus experiments, Foley [15,20] suggested that a range of primary lamproitic magmas from leucite lamproite to olivine lamproite can be derived by partial melting of phlogopite harzburgite as a function of pressure between <15 and >60 kbar. Mitchell [17] and Mitchell and Edgar [21] conducted liquidus experiments on Si-rich lamproites, and proposed considerably deeper melting of veins in the lithosphere (40–70 kbar). Finally, melting of subducted crustal material in the transition zone has been proposed by Murphy et al. [22] based on the interpretation of Pb isotopes.

Surprisingly, olivine is notably absent as a liquidus phase in all available liquidus experiments on silica-rich lamproites at the pressures in excess of 10 kbar, particularly when water is present [15,16]. This casts doubt on the phenocrystic origin of olivine, so that a xenocrystic origin, derived either from the mantle or from more Si-undersaturated rocks such as olivine-lamproites, picrites or komatiites became favoured [6,10–12]. An additional reason for this interpretation is its composition. Olivine with Fo >0.93 is very rare in nature, and is usually interpreted as being produced by extensive melting of peridotite mantle (>20%), which, however, results in much higher MgO concentration in the melt (up to 20% MgO) [23]. For such extensive melting, mantle peridotite requires temperatures above 1500 °C, which should be recorded in Cr_2O_3 in olivine of >0.2% and high whole-rock Ni contents of >500 ppm, as seen in komatiites and some picrites [24,25].

Our results provide important evidence that lamproitic olivines are of phenocrystic origin, and further support for relatively low extraction depths for Si-rich lamproites. The distribution of the data clearly

eliminates the possibility that the extremely Fo- and NiO enriched olivines could be mantle xenocrysts. Fig. 5 demonstrates that the majority of olivines from high-Si lamproites create an array which transects the region of mantle olivines and phenocrysts in picrites and komatiites (coloured regions in Fig. 5) at intermediate NiO and CaO with little overlap. This array is distinct from olivines that originate by other processes, and supports a phenocrystic origin for the high Fo, high NiO olivines. Picritic and komatiitic olivines crystallize from high-T melts produced by extensive melting of peridotite, and have considerably higher Cr_2O_3 content due to higher whole-rock chromium contents (Fig. 5), relative to lamproites (average 0.12%). The whole olivine population from Mediterranean lamproites, particularly Spanish, is polygenetic, partly originating as mantle xenocrysts and partly as high-Mg, high-Ni phenocrysts.

6.1.2. Extremely high NiO contents in olivine phenocrysts

Nickel is the most compatible trace element in olivine. As indicated by experimental studies, the partitioning of Ni between olivine and silicate melt increases with increasing Si/O and decreasing in MgO the melt [26,27]. This can be expressed in terms of the polymerisation of the melt by the proportion of bridging to non-bridging oxygen ions per tetrahedrally coordinated position in the melt (NBO/T). Lower amounts of non-bridging oxygen in the melt mean lower solubility and higher activity of the cation [28]. Olivine/melt partition coefficients for Ni are approximately linear functions of the NBO/T of the melt in the NBO/T=0.74–0.92 range [29].

Ni is universally reported as compatible in olivine, and $D_{Ni}^{Ol/liq}$ values reported mostly range between 7 and 11 [30,31] for anhydrous Si under-saturated basaltic compositions, whereas an increasing body of data indicate higher $D_{Ni}^{Ol/liq}$ for high SiO_2, low MgO compositions including boninites and high-Mg arc-related andesites [32,33], as well as lamproites [34], lamproitic ultrapotassic rocks [35] and alkaline Si-saturated and over-saturated rocks [36,37]. An additional factor may be the high alkali content (especially K), which may enable complexing of the transition elements in smaller structural units in the melt [34]. Although there is no experimental study of $D^{olivine/melt}$ as a function of alkali contents, Ni, Mn, Co, Cr and Zn show similar behaviour, not only in alkali and/or volatile-rich melts, but also in "normal" andesitic lavas (Fig. 6). Thus, Si/O and MgO in melts may be the major parameters which control $D^{olivine/melt}$ of these elements.

Our results for $D_{Ni}^{Ol/liq}$ in the Vera lavas yield values between 35 and 70, with an average of 40 (Table 2). We also recorded considerably higher partition coefficients for Mn, Co, Cr and Zn, relative to published values (Fig. 6). Our measurements are generally consistent with values for melts with similar NBO/T ratio (Fig. 6), which further corroborates compositional control of considerably higher partition coefficients for these trace elements. Accordingly, crystallization of olivines from high-Si and low-Mg alkaline melts is the best explanation for the extremely high $D_{Ni}^{Ol/liq}$ in the Vera lamproites. The very low CaO contents in olivine reflect the low level of CaO in the melt, as Ca in olivine is proposed to be an *in-situ* chemical potentiometer of the CaO activity in the melts [38]. This is derived from the ultra-depleted mantle component of the lamproitic mantle source.

All these arguments, taken together with experimental phase relations in the high-Si lamproites, are in accordance with low-pressure melting (10–20 kbar) of a depleted peridotite with a high contribution of orthopyroxene relative to olivine to the melt, giving rise to high-Si, relatively low magnesium melts. They oppose the notion that lamproites originate in the transition zone or lower mantle which has been proposed for Gaussberg and also for Spanish lamproites [22] on the basis of Pb isotope compositions. Both in Gaussberg [34] and in Spain, high $D_{Ni}^{Ol/liq}$ has been determined. If olivine had crystallized at high pressures, then trace element partition coefficients would be lower, as most partition coefficients decrease with increasing pressure, with Ni approaching a D of 1 at close to 15 GPa [39]. Furthermore, the melts would not show the high-SiO_2, refractory characteristics of the ultra-depleted peridotite component.

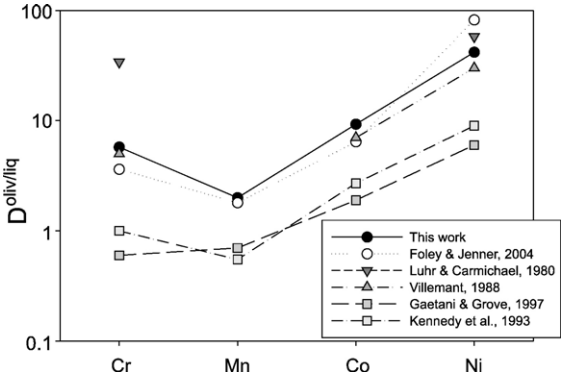

Fig. 6. Comparison of $D^{Ol/liquid}$ for Cr, Mn, Co and Ni determined in this study (filled circles) with literature data for Si-rich lamproites from Gaussberg [34], olivine-andesites from Colima volcano [36], trachybasalts from Phlegrean Fields [37], Si-undersaturated high-Mg melts produced experimentally by [80] and [31].

6.1.3. The ultra-depleted mantle component in the source of Mediterranean lamproites

Extremely high Fo olivine phenocrysts and their high-Cr spinel inclusions are a common feature of Mediterranean lamproites. As the first liquidus phases, they may present the only available proxy for the depleted mantle source component of lamproites, because the composition of the liquidus phases crystallizing from a primitive (i.e. unfractionated) magma should be close to that of residual phases in the mantle source. However, it must be considered that temperature, pressure, oxygen fugacity and the degree of partial melting may affect their chemistry and so confuse the proxy signal.

The extent of fractionation, and the effects of pressure, temperature and oxygen fugacity cannot be responsible for the extreme Mg# in olivine and Cr# in spinels found in Mediterranean lamproites. These parameters may explain high Cr# in spinel, but they cannot strongly influence the olivine composition, whereas fractionation and oxygen fugacity may cause the opposite effects. The best illustration is the coupling of Fo in olivine and Cr# in spinel on the OSMA diagram of Arai [40] (Fig. 7). Olivine–spinel pairs from Mediterranean lamproites partly plot in the most refractory part of the olivine–spinel mantle array (Fig. 7). A number of data plot off the array, defining variation trends for all Mediterranean lamproite provinces determined by low-pressure fractionation from positions in the most refractory part of the diagram.

The amount of partial melting is an important parameter which simultaneously influences the compositions of both spinel and olivine. In natural peridotites, the modal proportion of clinopyroxene gradually decreases and finally disappears in the course of partial melting, which is followed by an increase in the Cr# of spinel and Mg# of olivine. Although the lamproitic mantle source can be broadly defined (Section 6.1), it is not possible to define an overall degree of partial melting: the degree of melting will be higher in the vein than in the surrounding peridotite [18], but the majority of Si-rich lamproites are probably produced by less significant involvement of the wall-rock, otherwise all

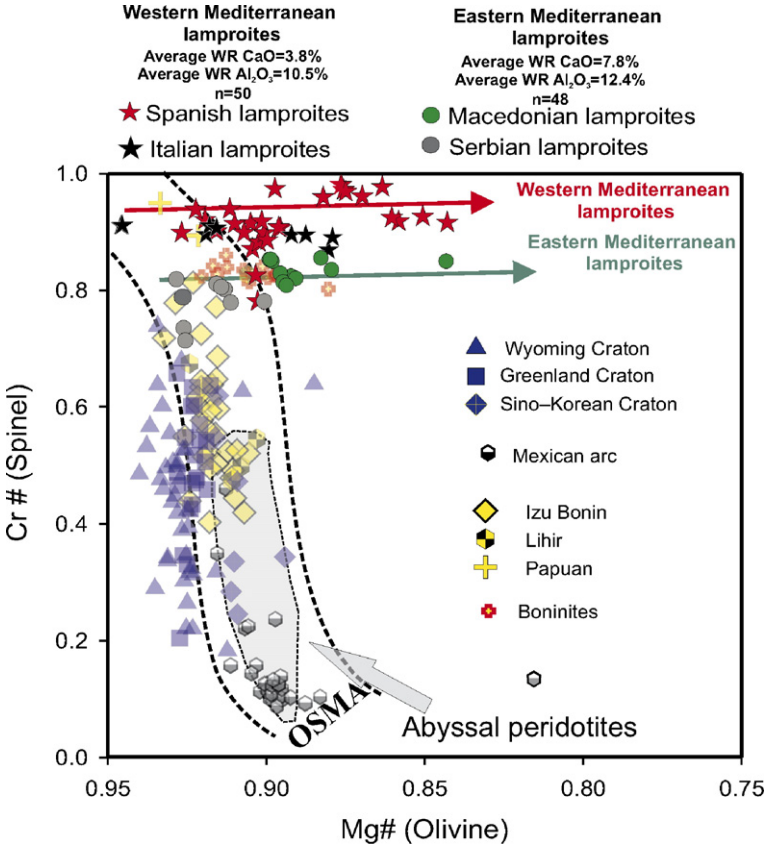

Fig. 7. Olivine–spinel pairs from the Mediterranean lamproites on the olivine–spinel mantle array (OSMA) diagram [40]. Data from Serbian lamproites from [9]. We compare them with the mineral pairs from mantle xenoliths from Wyoming, Greenland and Sino-Korean cratonic lithosphere [43–45], from abyssal peridotites [41], from Mexican lithosphere representing continental active margin [42], xenoliths from oceanic sub-arc mantle from Izu–Bonin and Lihir and Papuan ophiolites [46–48], and from boninite volcanics [51].

geochemical parameters derived from the vein would be diluted, causing melts to approach 45% SiO_2 and 15% of MgO, compositions rarely reported in the Mediterranean area [9]. Only high degrees of partial melting can simultaneously raise Fo in olivine and Cr# in spinel to reach extreme values.

The extent of depletion of the peridotitic mantle source component may be constrained using spinel and olivine pairs as a proxy [40]. The position of olivine–spinel pairs from primitive Mediterranean lamproites on Fig. 7 is more refractory than for mineral pairs from abyssal peridotites [41], mantle xenoliths from active continental margins [42] or for mantle xenoliths interpreted as relics of the Archaean lithosphere from the Wyoming, Greenland and Sino-Korean cratons [43–45]. Only some xenoliths from oceanic sub-arc mantle at Lihir, Papua New Guinea [46], and peridotites from the Izu–Bonin–Mariana forearc [47] or Papuan Ultramafic Belt [48] are similarly refractory.

When we compare our results with experimental melting studies in which the compositions of olivine and chromian spinel were monitored, these extremely refractory compositions appear to correspond to around 40 wt. % of previous melt extraction from pyrolite mantle [49,50]. Olivine–spinel pairs from lamproites are similarly or even more refractory than in boninites from Tonga trench [51]. Comparing lamproites with boninites, we may recognize similarities in MgO and SiO_2 contents and low CaO, Al_2O_3 and Na_2O contents, which have been interpreted as evidence for a strongly depleted mantle source for boninites and silica-rich lamproites of Mediterranean type [5]. Advancing the analogy with boninites [52,53], both boninites and lamproites have major element compositions (excluding high K_2O contents in lamproites) more similar to orthopyroxene than any other volcanic melt compositions. This clearly indicates the dominant role of orthopyroxene melting in the origin of both rock groups, which, together with the presence of water which is required to flux melting, further supports a low pressure origin for Si-rich lamproites [54].

Two important points emerge from our results. The first is a presence of a notable difference between lamproites from Spain and Italy (Western Mediterranean) relative to lamproites from the Balkans (Eastern Mediterranean) in terms of olivine–spinel pair compositions (Fig. 7). This is quite well correlated with the whole-rock Al_2O_3 and CaO contents; western Mediterranean lamproites have more refractory olivine–spinel pairs with generally lower CaO and Al_2O_3 contents, suggesting that the CaO and Al_2O_3 contents are controlled by the peridotitic component.

The second point is that the relation observed between Ol and Cr-spinel demands the contribution of an ultradepleted peridotite in lamproite melts, which contradicts models for lamproite genesis in which the melting of vein material is dominant, with negligible involvement of wall rock. It calls for a crucial role for ultradepleted peridotite, either during the vein+wall rock melting, or the passage of vein-derived melt through the harzburgite.

6.2. The origin of the ultra-depleted component and its geodynamic significance

As discussed above, the chemistry of liquidus lamproitic olivine and Cr-spinel reflects a high degree of depletion, providing essential information on the presence of ultra-depleted mantle component in their sources. Very low concentrations of CaO in Mediterranean lamproites are in accordance with the extremely refractory compositions of olivine–spinel pairs, indicating that Cpx had probably been eliminated from the mantle during previous melting episodes. Earlier studies of lamproites demonstrated that more than 20% of melts have been extracted during a previous depletion event in the garnet stability field [55]. Such characteristics are usually explained by komatiite extraction event(s) in the Archaean, reflecting the involvement of cratonic subcontinental lithosphere. However, mantle of such composition and age is unknown in ultramafic xenolith suites and tectonically emplaced ultramafic massifs of Western and Central Europe [56], and the oldest crust in Mediterranean is of Proterozoic age. Moreover, such a high extent of depletion is unknown from non-cratonic xenolith suites in continental intraplate regions, from orogenic massif peridotites of Phanerozoic age, nor even from convergent margins. Regarding the extent of depletion, oceanic arcs provide the only Phanerozoic mantle suites comparable to cratonic mantle [57].

Mediterranean lamproites occur in orogenic belts which mark the locus of continental convergence between African and Euroasian tectonic plates (Fig. 1). The Rif–Betic chain where Spanish lamproites occur is regarded as a collisional suture between Iberia and Africa, and consists of two superimposed orogenic belts [58]: (i) the External Betics are part of Alpine–Betic orogen, which originated during southeastward subduction of the European plate beneath the African plate. The orogen can be followed from the western Alps, Corsica, Tuscany to Calabria, and lamproitic volcanism occurs in most of these blocks; (ii) the Appenine–Maghrebides orogenic system, which is related to the late Oligocene–Pleistocene back-arc extension which took place in

response to Appenine subduction and arc rotation, forming the present-day arcuate geometry of the orogen. Recently, it has been suggested that the External Betics were located in a more north-eastern position as part of a continuation of the HP/LT Alpine–Betic orogen [59]. Fragments of the original orogenic belt have been rotated in response to Oligocene–Pleistocene subduction rollback.

In the central Balkans, lamproitic volcanism occurs exclusively in the Vardar zone and in eastern Serbia (Fig. 1), during distinct episodes in the Oligocene, Miocene and Pliocene [1,9], but not at all in neighbouring lithospheric blocks. The Vardar zone is an ophiolitic terrane representing the main suture zone of the Balkan Peninsula, consisting of a melange of peridotites, trench deposits, basalts and metamorphic soles [60]. Peridotites of the Vardar zone are mainly harzburgitic with very refractory olivine–spinel pairs [61], and the basalts are mostly comparable with those formed in a suprasubduction zone environment or in an island arc, including boninites [62,63]. Studies of ultramafic xenoliths hosted by Paleogene basanites in eastern Serbia [64,65] have shown that the lithospheric mantle beneath Serbia is more refractory than normal European lithosphere, and also significantly more depleted than most non-cratonic sub-continental mantle xenolith suites, orogenic peridotites and abyssal peridotites. The xenoliths are compositionally very similar to peridotites of modern oceanic sub-arc settings [65,66]. Moreover, a number of lower crustal xenoliths hosted by alkali basalts erupted during Alpine orogeny in the northern extension of the same suture zone, in Pannonian basin [67], have been interpreted as originating from the shallowest levels of ocean crust where pillow basalts are intimately intercalated with sediments, probably with a clastic input. This material would be accreted during subduction and convergence.

In both cases (Alpine–Betic orogen and Vardar zone), there is a clear relation between past subduction episodes and more recent lamproitic volcanism. Moreover, the

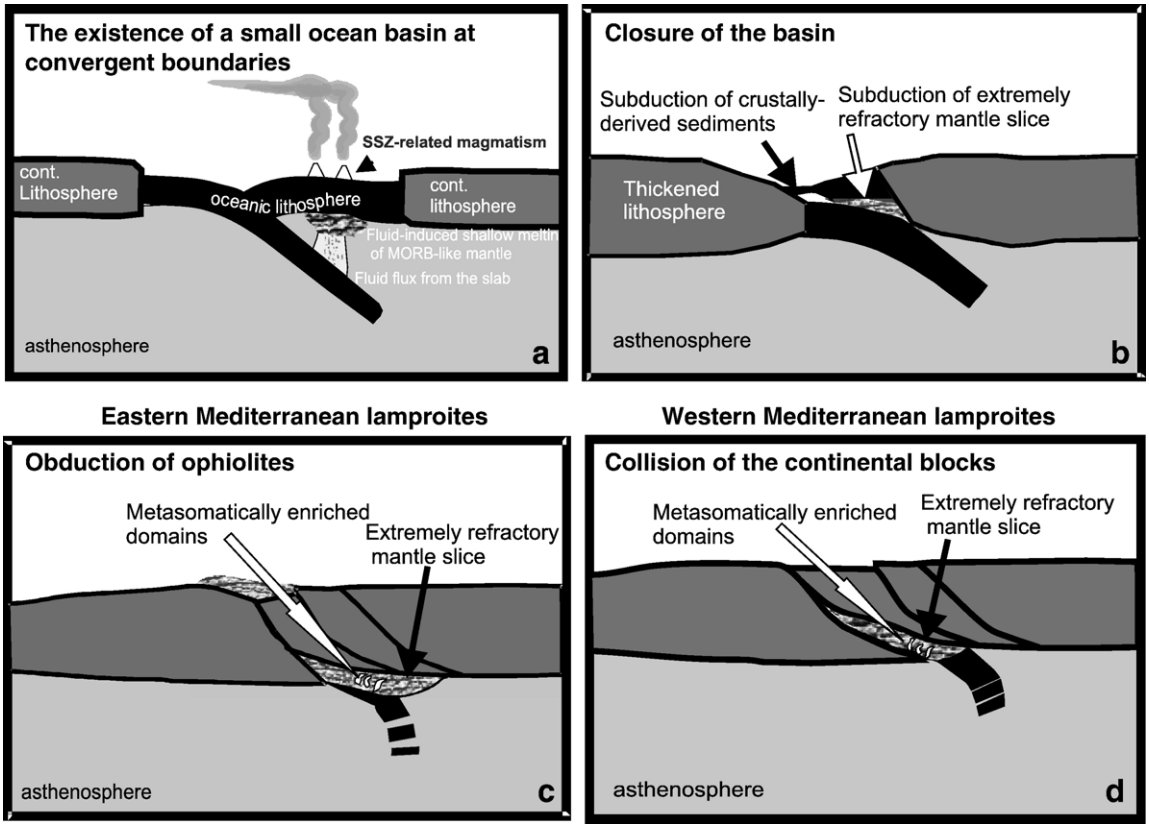

Fig. 8. A geodynamic scenario for the relationship between Mediterranean lamproites and plate convergence explaining the involvement of ultra-depleted uppermost mantle in lamproites. Closure of small ocean basins at convergent boundaries corresponds to events in Mediterranean Tethyan region during the Mesozoic, resulting in intraoceanic subduction (a, b). Supra-subduction volcanism leaves a strongly depleted uppermost mantle with high buoyancy relative to surrounding asthenosphere. Closure of the basin may be completed with either emplacement by obduction onto a passive margin (c) or accretionary uplift with continued collision (d). See the text for detailed explanations.

regional distribution of lamproites reflects the nature of the lithospheric mantle, as they occur exclusively in suture terrains geologically related with Mesozoic subduction events. This relationship has already been observed recently for the lamproites of Italy and Spain [7]. Ultra-depleted lithospheric mantle may have originated in a long-lived Andean-type subduction setting, which facilitated strong depletion in the continental mantle wedge prior to lamproite volcanism. However, there is no surviving evidence for such volcanism in the Mediterranean where lamproites occur. In the Western Alps, the Taveyanne Formation is comprised of resedimented volcanic material, occurring for several hundred km from eastern Switzerland (Glarus Alps) to the Western Alps in western Switzerland and France. However, the lower Oligocene age of the volcanic material [68] suggests a close relation to the contemporaneous Tertiary Periadriatic intrusions [69] including lamproites [70]. These age constrains clearly imply an essentially post-collisional character of both the lamproites and Taveayanne volcanics.

The strongly contrasting compositions of the ultra-depleted components in lamproitic sources raises the question of how old these ultra-depleted mantle blocks are and what such fragments are doing in a recent arc system. Potentially, the most promising way to constrain the depletion history of SCLM is by using Os isotope systematics. The highly compatible nature of Os relative to its parent Re, and its general immobility, make Os isotopes the most robust way to constrain the depletion age and history of SCLM. This, however, appears to be unsuccessful in the case of the ultrapotassic rocks: it has been shown that the most primitive ultrapotassic volcanics from Spain, Tibet, Navajo [71], Italy [72] and Serbia (Prelević, unpublished) have radiogenic Os isotopic compositions and are considerably enriched in elemental Os, eradicating any constraints about the depletion age of the mantle source. On the other hand, recent Os studies of some modern intraoceanic arc [73] and abyssal peridotites [74] report the presence of mantle fragments of diverse provenance, some showing ancient rhenium-depletion ages. Highly depleted peridotites are less dense and therefore less subductable than the fertile upper mantle. This may make oceanic subduction zones into near-surface graveyards for ancient oceanic lithosphere [73]. Similarly, hot and young subducting slabs that originated during short-lived periods of intraoceanic subduction are buoyant and likely to be obducted or accreted, constituting additions to continents.

Here, we propose a model which may explain the observed relation between the involvement of ultra-depleted mantle and the spatial distribution of lamproites. The most appropriate mantle source for the depleted component in the lamproites may resemble harzburgitic suprasubduction-type orogenic peridotites. Fig. 8a illustrates the general geodynamic situation during closure of a small ocean basin at a convergent boundary which approximates the events in the Mediterranean Tethyan region during Mesozoic times. The origin of suprasubduction zone (SSZ) arc-related melts is debated, but it is plausible that they are formed at the initiation of subduction [75]. If we regard the intraoceanic suprasubduction peridotites in the simplest way, we may assume that they underwent twofold depletion: first during the production of MORB, and secondly associated with intraoceanic subduction to produce a spectrum of arc-related melts. Other models suggest subduction of mid-ocean ridges or the influence of plumes (for boninites) [76], but in all cases, the inferred melting conditions correspond to shallow and hydrous melting of strongly depleted upper mantle. Moreover, recent studies [47] demonstrated that oceanic sub-arc mantle lithosphere may have undergone extensive interaction with subduction-derived magmas (boninites), which may additionally amplify its depleted signature.

The closure of small ocean basins may be facilitated by intraoceanic subduction (Fig. 8a, b) which was probably common during Mesozoic Mediterranean Tethyan geodynamics [77]. SSZ-related volcanism would leave a strongly depleted mantle area which should be buoyant relative to surrounding asthenosphere. Closure of the basin may therefore be completed with emplacement by obduction of buoyant material onto a passive margin (Fig. 8c), which we propose for the Eastern Mediterranean lamproites, or by its accretionary uplift with continued collision (Fig. 8d), which is more suitable for the Western Mediterranean lamproites. This model is especially suitable for the Eastern Mediterranean, where the closure of small oceanic branches of the Tethys ocean often led to the obduction of ophiolites [77].

Our model considers only one, ultra-depleted, component in lamproite genesis. However, stacking of arc-oceanic mantle blocks may involve crust-derived sediments (Fig. 8c, d), so that they may be intimately intermixed with depleted peridotites during the closure of small oceanic basins, explaining why the highly enriched component of Mediterranean lamproites is typically crustal [9]. According to our model, depleted slices of oceanic mantle have been also heavily metasomatised by the subsequent interaction

with melts or fluids derived from the melting of crustal sediments. Harzburgitic peridotite is known to be preferentially affected by metasomatic enrichment processes. The process of melting of crustal material interlayered with depleted peridotite is very similar to that modelled by Sekine and Wyllie [78] and Wyllie and Sekine [79]. The melt is silica-rich and must react with the peridotite in an incongruent reaction that forms Phl+Opx+Cpx and consumes olivine, increasing the abundance of Opx in the source area. Later, lithosphere delamination (in Tertiary) caused by orogen collapse may initiate remelting of such domains and further reaction with the peridotite host [1].

Acknowledgements

We thank Mathias Barth for his assistance with LAM-ICP-MS analyses at the University of Mainz. The manuscript was improved through discussions with Gideon Rosenbaum, Vladica Cvetković, Mathias Barth, Sebastian Tappe and Jovanović Zoran. D.P. is especially grateful to H. Downes for essential discussions in the early phases of the study. Reviews by four anonymous reviewers considerably improved the clarity of our argumentation, and are gratefully acknowledged. Rick Carlson helped to refine the final form of the manuscript. This work was supported through the Deutsche Forschungsgemeinschaft (DFG) within the project Fo 181/18-1.

Appendix A

Laser Ablation ICP-MS results for USGS BCR2-G compared to averaged published data. All data in ppm

Element	035BCR2G	007BCR2G	020BCR2G	021BCR2G	020BCR2	Average	Recommended*
Li	10.5	9.99	9.19	9.79	10.01	9.90	9.21
Sc	30.09	29.9	30.16	28.91	29.9	29.79	33.24
Ti	14,306	13,106	13,147	12,836	14,913	13,662	13,678
V	423.34	425.03	416.54	412.91	398.91	415.35	418.92
Cr	19.61	17.04	16.79	17.43	15.29	17.23	16.64
Mn	1560	1475	1432	1438	1539	1489	1529
Co	37.49	36.14	35.94	36.69	37.31	36.71	38.33
Ni	11.9	11.26	10.77	11.76	12.24	11.59	14.19
Cu	16.39	14.49	14.54	15.67	18.21	15.86	21.40
Zn	159.27	128.79	147.35	149.64	173.68	151.75	134.45
Ga	31.63	34.06	34.46	33.99	37.29	34.29	32.85
Sr	314.6	303.26	309.41	300.44	294.13	304.37	334.52
Y	27.79	26.98	28.6	28.03	26.95	27.67	34.55
Zr	145.7	139.81	149.09	144.34	138.94	143.58	186.81
Nb	11.51	11.15	11.39	10.97	11.41	11.29	13.15
Ba	645.96	621.39	632.32	622.01	605.84	625.50	669.85
Ce	51.49	49.61	50.3	49.51	48.37	49.86	51.62
Yb	3.14	3.03	3.07	3.01	2.93	3.04	3.36
Hf	3.95	3.77	4.02	3.97	3.7	3.88	4.87
Ta	0.71	0.68	0.70	0.68	0.69	0.69	0.78

*Averages of published data for USGS BCR2-G from GeoREM database (http://georem.mpch-mainz.gwdg.de/).

Appendix B. Supplementary data

Supplementary data associated with this article can be found, in the online version, at doi:10.1016/j.epsl.2007.01.018.

References

[1] D. Prelević, S.F. Foley, V. Cvetković, A review of petrogenesis of Mediterranean Tertiary lamproites: a perspective from the Serbian ultrapotassic province, in: L. Beccaluva, G. Bianchini, M. Wilson (Eds.), Cenozoic Volcanism in the Mediterranean Area, Geological Society of America Special Paper, vol. 418, 2007, pp. 113–129.

[2] D.R. Nelson, Isotopic characteristics of potassic rocks: evidence for the involvement of subducted sediments in magma genesis, Lithos 28 (1992) 403–420.

[3] D.R. Nelson, M.T. McCulloch, S.S. Sun, The origins of ultrapotassic rocks as inferred from Sr, Nd and Pb isotopes, Geochim. Cosmochim. Acta 50 (1986) 231–245.

[4] S.F. Foley, G. Venturelli, D.H. Green, L. Toscani, The ultrapotassic rocks: characteristics, classification and constraints for petrogenetic models, Earth-Sci. Rev. 24 (1987) 81–134.

[5] S.F. Foley, G. Venturelli, High K_2O rocks with high MgO, high SiO_2 affinities, in: A.J. Crawford (Ed.), Boninites and Related Rocks, Unwin Hyman, London, 1989, pp. 72–88.

[6] R.H. Mitchell, S.C. Bergman, Petrology of Lamproites, Plenum Press, New York, 1991 447 pp.
[7] A. Peccerillo, G. Martinotti, The Western Mediterranean lamproitic magmatism: origin and geodynamic significance, Terra Nova 18 (2006) 109–117.
[8] S. Conticelli, L. Melluso, G. Perini, R. Avanzinelli, E. Boari, Petrologic, Geochemical and Isotopic Characteristics of Potassic and Ultrapotassic Magmatism in Central-Southern Italy; Inferences on its Genesis and on the Nature of Mantle Sources, A Showcase of the Italian Research in Petrology; Magmatism in Italy, vol. 73; Special issue 1, Bardi Editore, Rome, Italy, 2004, pp. 135–164.
[9] D. Prelević, S.F. Foley, R.L. Romer, V. Cvetković, H. Downes, Tertiary ultrapotassic volcanism in Serbia: constraints on petrogenesis and mantle source characteristics, J. Petrol. 46 (2005) 1443–1487.
[10] G. Carlier, J.-P. Lorand, Petrogenesis of a zirconolite-bearing Mediterranean-type lamproite from the Peruvian Altiplano (Andean Cordillera), Lithos 69 (2003) 15–35.
[11] D. Velde, Armalcolite–Ti–phlogopite–diopside–analcite-bearing lamproites from Smoky Butte, Garfield County, Montana, Am. Mineral. 60 (1975) 566–573.
[12] Y. Xu, X. Huang, M.A. Menzies, R. Wang, Highly magnesian olivines and green-core clinopyroxenes in ultrapotassic lavas from western Yunnan, China: evidence for a complex hybrid origin, Eur. J. Mineral. 15 (2003) 965–975.
[13] N.J.G. Pearce, W.T. Perkins, J.A. Westgate, M.P. Gorton, S.E. Jackson, C.R. Neal, S.P. Chenery, A compilation of new and published major and trace element data for NIST SRM 610 and NIST SRM 612 glass reference materials, Geostand. Newsl. 21 (1997) 115–144.
[14] G. Venturelli, S. Capedri, G.D. Battistini, A. Crawford, L. Kogarko, S. Celestini, The ultrapotassic rocks from southeastern Spain, Lithos 17 (1984) 37–54.
[15] S.F. Foley, The genesis of lamproitic magmas in a reduced fluorine-rich mantle, in: J. Ross, A.L. Jacques, J. Ferguson, D.H. Green, S.Y. O'Reilly, R.V. Danchin, A.J.A. Janse (Eds.), Fourth International Kimberlite Conference Special Publication Number 14, vol. 1, Geological Society of Australia, Perth, 1989, pp. 616–631.
[16] S.F. Foley, Petrological characterization of the source components of potassic magmas: geochemical and experimental constraints, Lithos 28 (1992) 187–204.
[17] R.H. Mitchell, Melting experiments on a sanidine phlogopite lamproite at 4–7 GPa and their bearing on the sources of lamproitic magmas, J. Petrol. 36 (1995) 1455–1474.
[18] S.F. Foley, Vein-plus-wall-rock melting mechanisms in the lithosphere and the origin of potassic alkaline magmas, Lithos 28 (1992) 435–453.
[19] S.F. Foley, D.S. Musselwhite, S.R. van der Laan, in: J.J. Gurney, J.L. Gurney, M.D. Pascoe, S.H. Richardson (Eds.), Melt Compositions from Ultramafic Vein Assemblages in the Lithospheric Mantle: a Comparison of Cratonic and Non-Cratonic Settings, The J B Dawson Volume, Proceedings of the VIIth International Kimberlite Conference, vol. 17, Red Roof Design, Capetown, 1999, pp. 238–246.
[20] S.F. Foley, An experimental study of olivine lamproite-first results from the diamond stability field, Geochim. Cosmochim. Acta 57 (1993) 483–489.
[21] R.H. Mitchell, A.D. Edgar, Melting experiments on SiO_2-rich lamproites to 6.4 GPa and their bearing on the sources of lamproite magmas, Mineral. Petrol. 74 (2002) 115–128.
[22] D.T. Murphy, K.D. Collerson, B.S. Kamber, Lamproites from Gaussberg, Antarctica: possible transition zone melts of Archaean subducted sediments, J. Petrol. 43 (2002) 981–1001.
[23] N.T. Arndt, Komatiites, kimberlites, and boninites, J. Geophys. Res. 108 (B6) (2005) 2293.
[24] N.T. Arndt, A.J. Naldrett, D.R. Pyke, Komatiitic and iron-rich tholeiitic lavas of Munro Township, Northeast Ontario, J. Petrol. 18 (1977) 319–369.
[25] I.H. Campbell, Identification of ancient mantle plumes, in: R. Ernst, K.L. Buchan (Eds.), Mantle Plumes, Their Identification through Time, vol. 352, Geological Society of America (GSA), Boulder, CO, United States, 2001, pp. 5–21.
[26] S. Hart, K. Davies, Nickel partitioning between olivine and silicate melt, Earth Planet. Sci. Lett. 40 (1978) 203–219.
[27] R.J. Kinzler, T.L. Grove, S.I. Recca, An experimental study on the effect of temperature and melt composition on the partitioning of nickel between olivine and silicate melt, Geochim. Cosmochim. Acta 54 (1990) 1255–1265.
[28] B.O. Mysen, E.V. Dubinsky, Melt structural control on olivine/melt element partitioning of Ca and Mn, Geochim. Cosmochim. Acta 68 (2004) 1617–1633.
[29] B.O. Mysen, D. Virgo, Trace element partitioning and melt structure: an experimental study at 1 atm pressure, Geochim. Cosmochim. Acta 44 (1980) 1917–1930.
[30] T. Dunn, C. Sen, Mineral/matrix partition coefficients for orthopyroxene, plagioclase, and olivine in basaltic to andesitic systems: a combined analytical and experimental study, Geochim. Cosmochim. Acta 58 (1994) 717–733.
[31] A.K. Kennedy, G.E. Lofgren, G.J. Wasserburg, An experimental study of trace element partitioning between olivine, orthopyroxene and melt in chondrules: equilibrium values and kinetic effects, Earth Planet. Sci. Lett. 115 (1993) 177–195.
[32] M. Nakamura, Residence time and crystallization history of nickeliferous olivine phenocrysts from the northern Yatsugatake volcanoes, Central Japan: application of a growth and diffusion model in the system Mg–Fe–Ni, J. Volcanol. Geotherm. Res. 66 (1995) 81–100.
[33] V.S. Kamenetsky, A.J. Crawford, S. Eggins, R. Muhe, Phenocryst and melt inclusion chemistry of near-axis seamounts, Valu Fa Ridge, Lau Basin: insight into mantle wedge melting and the addition of subduction components, Earth Planet. Sci. Lett. 151 (1997) 205–223.
[34] S.F. Foley, G.A. Jenner, Trace element partitioning in lamproitic magmas — the Gaussberg olivine leucitite, Lithos 75 (2004) 19–38.
[35] L.L. Davis, D. Smith, Ni-rich olivine in minettes from Two Buttes, Colorado: a connection between potassic melts from the mantle and low Ni partition coefficients, Geochim. Cosmochim. Acta 57 (1993) 123–129.
[36] J.F. Luhr, I.S.E. Carmichael, The Colima volcanic complex, Mexico: I. Post-caldera andesites from Volcan Colima, Contrib. Mineral. Petrol. 71 (1980) 343–372.
[37] B. Villemant, Trace element evolution in the Phlegrean Fields (Central Italy): fractional crystallization and selective enrichment, Contrib. Mineral. Petrol. 98 (1988) 169–183.
[38] G. Libourel, Systematics of calcium partitioning between olivine and silicate melt: implications for melt structure and calcium content of magmatic olivines, Contrib. Mineral. Petrol. 136 (1999) 63–80.
[39] E.A. McFarlane, M.J. Drake, Element partitioning and the early thermal history of the Earth, in: J.H. Jones, H.E. Newsom (Eds.), Origin of the Earth, Oxford Univ. Press, New York, NY, United States, 1990, pp. 135–150.
[40] S. Arai, Characterization of spinel peridotites by olivine–spinel compositional relationships: review and interpretation, Chem. Geol. 113 (1994) 191–204.

[41] H.J.B. Dick, T. Bullen, Chromian spinel as a petrogenetic indicator in abyssal and alpine-type peridotites and spatially associated lavas, Contrib. Mineral. Petrol. 86 (1984) 54–76.
[42] J.F. Luhr, J.J. Aranda-Gomez, Mexican peridotite xenoliths and tectonic terranes: correlations among vent location, texture, temperature, pressure, and oxygen fugacity, J. Petrol. 38 (1997) 1075–1112.
[43] S. Bernstein, P.B. Kelemen, C.K. Brooks, Depleted spinel harzburgite xenoliths in Tertiary dykes from East Greenland: restites from high degree melting, Earth Planet. Sci. Lett. 154 (1998) 221–235.
[44] J. Zheng, S.Y. O'Reilly, W.L. Griffin, F. Lu, M. Zhang, N.J. Pearson, Relict refractory mantle beneath the eastern North China block: significance for lithosphere evolution, Lithos 57 (2001) 43–66.
[45] H. Downes, R. Macdonald, B.G.J. Upton, K.G. Cox, J.-L. Bodinier, P.R.D. Mason, D. James, P.G. Hill, B.C. Hearn Jr., Ultramafic xenoliths from the Bearpaw Mountains, Montana, USA: evidence for multiple metasomatic events in the lithospheric mantle beneath the Wyoming Craton, J. Petrol. 45 (2004) 1631–1662.
[46] B.I.A. McInnes, M. Gregoire, R.A. Binns, P.M. Herzig, M.D. Hannington, Hydrous metasomatism of oceanic sub-arc mantle, Lihir, Papua New Guinea: petrology and geochemistry of fluid-metasomatised mantle wedge xenoliths, Earth Planet. Sci. Lett. 188 (2001) 169–183.
[47] I.J. Parkinson, J.A. Pearce, Peridotites from the Izu–Bonin–Mariana Forearc (ODP Leg 125): evidence for mantle melting and melt–mantle interaction in a supra-subduction zone setting, J. Petrol. 39 (1998) 1577–1618.
[48] A.L. Jaques, B.W. Chappell, Petrology and trace element geochemistry of the Papuan Ultramafic Belt, Contrib. Mineral. Petrol. 75 (1980) 55–70.
[49] K.N. Matsukage, K. Kubo, Chromian spinel during melting experiments of dry peridotite (KLB-1) at 1.0–2.5 GPa, Am. Mineral. 88 (2003) 1271–1278.
[50] A.L. Jaques, D.H. Green, Anhydrous melting of peridotite at 0–15 kbar pressure and the genesis of tholeiitic basalts, Contrib. Mineral. Petrol. 73 (1980) 287–310.
[51] A.V. Sobolev, L.V. Danyushevsky, Petrology and geochemistry of boninites from the north termination of the Tonga Trench: constraints on the generation conditions of primary high-Ca boninite magmas, J. Petrol. 35 (1994) 1183–1211.
[52] V.S. Kamenetsky, A.J. Crawford, S. Meffre, Factors controlling chemistry of magmatic spinel: an empirical study of associated olivine, Cr-spinel and melt inclusions from primitive rocks, J. Petrol. 42 (2001) 655–671.
[53] V.S. Kamenetsky, A.V. Sobolev, S.M. Eggins, A.J. Crawford, R.J. Arculus, Olivine-enriched melt inclusions in chromites from low-Ca boninites, Cape Vogel, Papua New Guinea: evidence for ultramafic primary magma, refractory mantle source and enriched components, in: E.H. Hauri, A.J.R. Kent, N. Arndt (Eds.), Melt Inclusions at the Millennium: Toward a Deeper Understanding of Magmatic Processes, vol. 183, Elsevier, Amsterdam, Netherlands, 2002, pp. 287–303.
[54] S.R. Van der Laan, M.F.J. Flower, V.G.A.F. Koster, Experimental evidence for the origin of boninites: near-liquidus phase relations to 7.5 kbar, in: A.J. Crawford (Ed.), Boninites, Unwin Hyman, London, 1989, pp. 112–147.
[55] K.M. Tainton, D. McKenzie, The generation of kimberlites, lamproites, and their source rocks, J. Petrol. 35 (1994) 787–817.
[56] H. Downes, Formation and modification of the shallow sub-continental lithospheric mantle: a review of geochemical evidence from ultramafic xenolith suites and tectonically emplaced ultramafic massifs of Western and Central Europe, J. Petrol. 42 (2001) 233–250.
[57] F.R. Boyd, Compositional distinction between oceanic and cratonic lithosphere, Earth Planet. Sci. Lett. 96 (1989) 15–26.
[58] C. Doglioni, E. Gueguen, F. Sabat, M. Fernandez, The Western Mediterranean extensional basins and the Alpine orogen, Terra Nova 9 (1997) 109–112.
[59] G. Rosenbaum, G.S. Lister, Formation of arcuate orogenic belts in the western Mediterranean region, in: A.J. Sussman, A.B. Weil (Eds.), Orogenic Curvature: Integrating Paleomagnetic and Structural Analyses Special Paper, vol. 383, Geological Society of America, Boulder, CO, 2004, pp. 41–56.
[60] S. Karamata, N.M. Dimitrijević, D.M. Dimitrijević, Oceanic realms in the central part of the Balkan Peninsula during the Mesozoic, Slovak Geol. Mag. 5 (1999) 173–177.
[61] Z. Maksimović, L. Kolomejceva-Jovanović, Sastav koegzistentnih minerala peridotita Jugoslavije i problemi geotermometrije i geobarometrije ultramafitskih zona, Glas SANU, Odeljenje prirodno-matematièkih nauka, vol. 51, 1987, pp. 21–52.
[62] A.H.F. Robertson, S. Karamata, The role of subduction–accretion processes in the tectonic evolution of the Mesozoic Tethys in Serbia, Tectonophysics 234 (1994) 73–94.
[63] M. Marroni, L. Pandolfi, E. Saccani, M. Zelić, Boninites from the Kopaonik area (Southern Serbia): new evidences for suprasubduction ophiolites in the Vardar zone, Ofioliti 29 (2004) 251–254.
[64] V. Cvetković, H. Downes, D. Prelević, M. Jovanović, M. Lazarov, Characteristics of the lithospheric mantle beneath East Serbia inferred from ultramafic xenoliths in Paleogene basanites, Contrib. Mineral. Petrol. 148 (2004) 335–357.
[65] V. Cvetković, M. Lazarov, H. Downes, D. Prelević, Modification of the subcontinental mantle beneath East Serbia: evidence from orthopyroxene-rich xenoliths, Lithos, Corrected Proof (In Press).
[66] V. Cvetković, H. Downes, D. Prelević, M. Lazarov, K. Resimić-Šarić, Geodynamic significance of ultramafic xenoliths from Eastern Serbia: relics of sub-arc oceanic mantle? Journal of Geodynamics, Corrected Proof (In Press).
[67] G. Dobosi, P. Kempton, H. Downes, A. Embey-Isztin, M. Thirlwall, P. Greenwood, Lower crustal granulite xenoliths from the Pannonian Basin, Hungary, Part 2: Sr–Nd–Pb–Hf and O isotope evidence for formation of continental lower crust by tectonic emplacement of oceanic crust, Contrib. Mineral. Petrol. 144 (2003) 671–683.
[68] R. Ruffini, M.A. Cosca, A. d'Atri, J.C. Hunziker, R. Polino, The volcanic supply of the Taveyanne turbidites (Savoie, France): a riddle for Tertiary Alpine volcanism, Accad. Naz. Scienze detta dei XL, Roma, Atti convegno Rapporti Alpi-Appennino, 1995, pp. 359–376.
[69] G.V. Dal Piaz, G. Venturelli, Brevi riflessioni sul magmatismo post-ofiolitico nel quadro dell'evoluzione spazio-temporale delle Alpi, Mem. Soc. Geol. Ital. 26 (1983) 5–19.
[70] G. Venturelli, R. Thorpe, G.D. Piaz, A.D. Moro, P. Potts, Petrogenesis of calk-alkaline, shoshonitic and associated ultrapotassic Oligocene volcanic rocks from the Northwestern Alps, Italy, Contrib. Mineral. Petrol. 86 (1984) 209–220.
[71] B.F. Schaefer, S.P. Turner, N.W. Rogers, C.J. Hawkesworth, H.M. Williams, D.G. Pearson, G.M. Nowell, Re–Os isotope characteristics of postorogenic lavas; implications for the nature of young lithospheric mantle and its contribution to basaltic magmas, Geology (Boulder) 28 (2000) 563–566.
[72] S. Conticelli, R.W. Carlson, E. Widom, G. Serri, Os, Sr, Nd and Pb isotope composition of Italian Quaternary volcanism, in: L.

Beccaluva, G. Bianchini, M. Wilson (Eds.), Cenozoic Volcanism in the Mediterranean Area: Geological Society of America Special Paper, vol. 418, 2007, In Print.

[73] I.J. Parkinson, C.J. Hawkesworth, A.S. Cohen, Ancient mantle in a modern arc: osmium isotopes in Izu–Bonin–Mariana Forearc peridotites, Science 281 (1998) 2011–2013.

[74] J. Harvey, A. Gannoun, K.W. Burton, N.W. Rogers, O. Alard, I.J. Parkinson, Ancient melt extraction from the oceanic upper mantle revealed by Re–Os isotopes in abyssal peridotites from the Mid-Atlantic ridge, Earth Planet. Sci. Lett. 244 (2006) 606–621.

[75] R.J. Stern, S.H. Bloomer, Subduction zone infancy; examples from the Eocene Izu–Bonin–Mariana and Jurassic California arcs, Geol. Soc. Amer. Bull. 104 (1992) 1621–1636.

[76] A.J. Crawford, T.J. Falloon, D.H. Green, Classification, petrogenesis and tectonic setting of boninites, in: A.J. Crawford (Ed.), Boninites, Unwin Hyman, London, 1989, pp. 1–49.

[77] A.H.F. Robertson, Overview of the genesis and emplacement of Mesozoic ophiolites in the Eastern Mediterranean Tethyan region, Lithos 65 (2002) 1–67.

[78] T. Sekine, P.J. Wyllie, Phase relationships in the system $KAlSiO_4$–Mg_2SiO_4–SiO_2–H_2O as a model for hybridization between hydrous siliceous melts and peridotite, Contrib. Mineral. Petrol. 79 (1982) 368–374.

[79] P.J. Wyllie, T. Sekine, The formation of mantle phlogopite in subduction zone hybridization, Contrib. Mineral. Petrol. 79 (1982) 375–380.

[80] G.A. Gaetani, T.L. Grove, Partitioning of moderately siderophile elements among olivine, silicate melt, and sulfide melt: constraints on core formation in the Earth and Mars, Geochim. Cosmochim. Acta 61 (1997) 1829–1846.